J. Fluid Mech. (1992), *vol.* 236, *pp.* 665–689
Printed in Great Britain

Two-dimensional vortex-dipole interactions in a stratified fluid

By S. I. VOROPAYEV AND YA. D. AFANASYEV
Institute of Oceanology, USSR Academy of Sciences, Krasikova 23, Moscow 117218, USSR

(Received 13 July 1990 and in revised form 16 September 1991)

Planar motion produced when a viscous fluid is forced from an initial state of rest is studied. We consider a vortex dipole produced by the action of a point force (Cantwell 1986), and a vortex quadrupole produced by the action of two equal forces of opposite direction. We also present results from an experimental investigation into the dynamics of the interactions between vortex dipoles as well as between vortex dipoles and a vertical wall in a stratified fluid. Theoretical consideration reveals that the dynamics of two-dimensional vortex-dipole interactions are determined by two main governing parameters: the dipolar intensity of the vorticity distribution (momentum) and the quadrupolar intensity of the vorticity distribution of the flow. We document details of different basic types of interactions and present a physical interpretation of the results obtained in terms of vortex multipoles: dipoles, quadrupoles and their combinations.

1. Introduction

Various irregular quasi-two-dimensional flows associated with the term 'two-dimensional turbulence' are induced by a system of forces applied to a fluid. The stratified ocean, where gravity suppresses motion in the vertical direction, is a typical geophysical example of a nearly two-dimensional system where various natural factors act as irregular forces. These forces generate vortex motions of different horizontal scales. Noticeable among them are the mesoscale (30–100 km) vortex structures: vortices, eddies, rings. The interactions of these structures with each other and also with coastal ridges strongly influence the instantaneous fields of velocity, temperature and salinity in the ocean and determine oceanic 'weather'. In the last few years examples of a new form of mesoscale vortex structure, named the mushroom-like current (Fedorov & Ginzburg 1989), have been observed in great numbers in visual and infrared satellite images of the upper ocean. A typical mushroom-like current is a system of two vortices of opposite sign (vortex dipole) which can be considered as the simplest compact vortex structure which has momentum. It is clear that for some volume of fluid to acquire a momentum, some localized external (or internal) force must be applied to the fluid. The action of a localized force plus the action of gravity leads to vortex dipole formation in a stratified upper ocean. It seems that vortex dipoles and also their combinations (e.g. vortex quadrupoles) are the universal product of any irregular forcing in two-dimensional flows. Theoretical analysis (Manakov & Schur 1983) of a system of point vortices in an ideal fluid demonstrates that an isolated vortex in that system cannot remain single asymptotically. Isolated vortices of different sign form dipoles of zero total circulation. The dipole has a momentum and hence it can be considered as an elementary 'particle' in two-dimensional fluid dynamics.

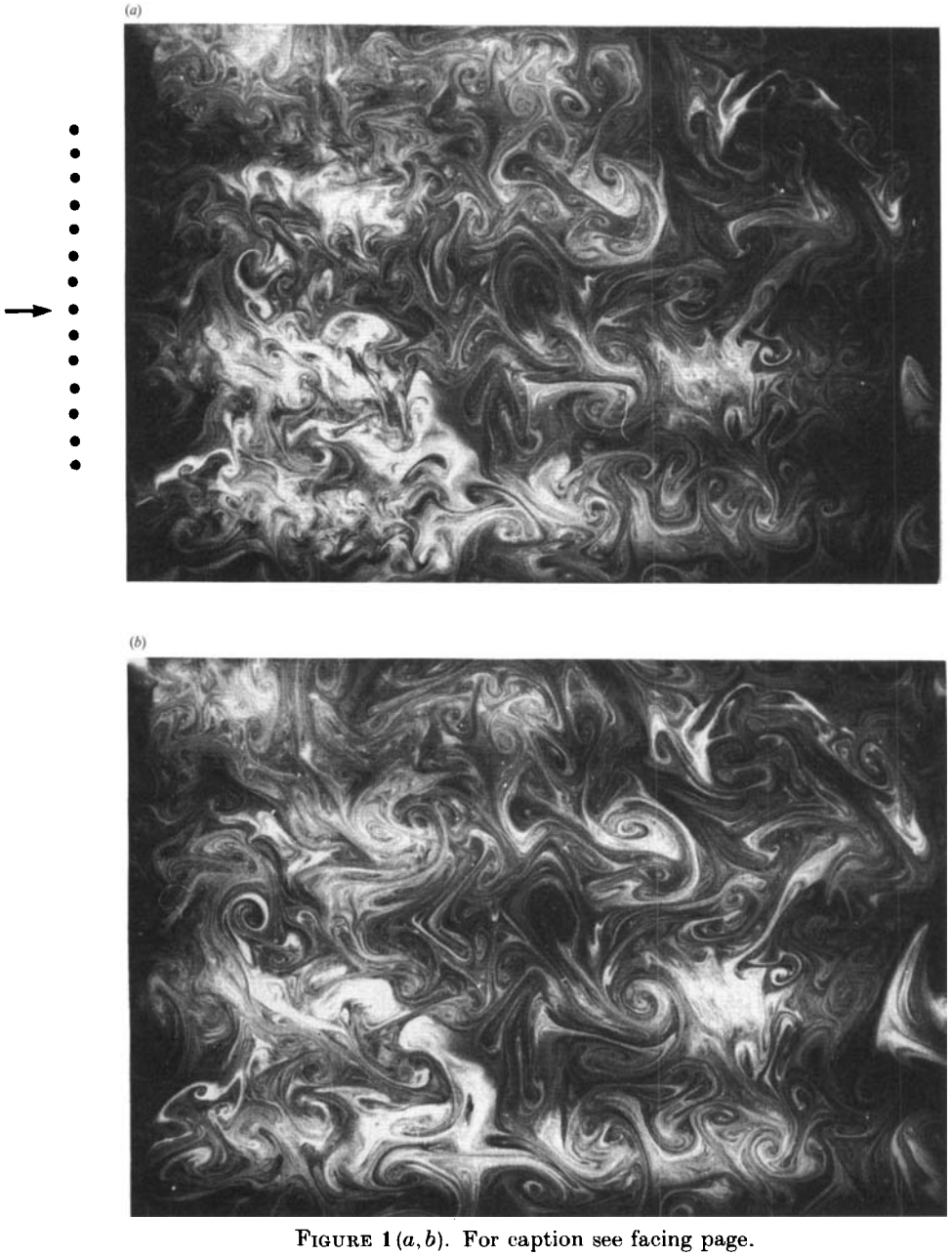

FIGURE 1 (*a*, *b*). For caption see facing page.

To illustrate specific features of the flow induced in a stratified fluid by a system of forces, consider a simple experiment. A thin layer (0.5 cm depth) of dyed fresh water lies on a layer of salt water. We move a row of vertical bars (diameter 0.05 cm, mesh 1 cm) back and forth in horizontal directions in the upper layer, thus applying localized external forces. Figure 1 shows the subsequent development of the flow induced. One can see clearly in this sequence that the fundamental elements of the flow are not single vortices but vortex dipoles. For impulsive force action, shown in figure 1, a small-scale motion rapidly decays and numerous large-scale dipoles

FIGURE 1 (*a–d*). Photographic sequence showing a top view of the evolution of numerous dipole-like coherent structures in an initially ($t = 0$) turbulent upper layer of density-stratified water. The lengthscale of the motion (typical diameter of the dipoles) is approximately ten times greater than the depth of the upper layer and increases with time as $R \propto t^{\frac{1}{2}}$: (*a*) $t = 2$ s, (*b*) 8 s, (*c*) 36 s, (*d*) 98 s. The row of points to the left of the first photograph represent the horizontal cross-section of the vertical bars, the arrow shows the direction of motion of the bars.

appear. As a result of dipole interactions and viscous diffusion, the lengthscales of the dipoles increase with time as $R \propto t^{\frac{1}{2}}$. The nature of the forces inducing the motion is not important here. Similar, numerous dipolar structures are clearly seen in Griffiths & Hopfinger (1984, photos 2, 3) who studied experimentally mesoscale turbulence

generated by baroclinic instability. The forces inducing the motion in that case were internal. Other examples include flows in a soap film (Couder & Basdevant 1986), or in a layer of mercury in a magnetic field (Nguen Duc & Sommeria 1988).

Before investigating a complicated irregular flow of the sort shown in figure 1, it seems reasonable to reproduce and to study an isolated dipole with controllable characteristics in a stratified fluid. This simple idea was exploited in laboratory experiments, where laminar (Voropayev 1983) or turbulent (Voropayev 1987) horizontal jets from a thin round nozzle were used as controllable sources of momentum. In both cases, a compact vortex dipole was easily generated in a stratified fluid. Later, different aspects of isolated vortex-dipole dynamics were studied experimentally by van Heijst & Flor (1989*a*, *b*), Afanasyev & Voropayev (1989*a*) and Afanasyev, Voropayev & Filippov (1988, 1989), numerically by Voropayev & Neelov (1991), and theoretically by Barenblatt, Voropayev & Fillipov (1989) and Afanasyev & Voropayev (1989*b*). The characteristics of isolated vortex dipoles in a stratified fluid have been well studied and they are summarized in a detailed paper by Voropayev, Afanasyev & Fillipov (1991).

The next, natural step in studies of vortex-dipole dynamics in a stratified fluid is the investigation of more complicated vortex structures, which appear as a result of the interaction of dipoles with each other and with a boundary. Preliminary experiments on the head-on collision of two impulsive strong jets in a stratified fluid have demonstrated the appearance of an unsteady vortex quadrupole (Afanasyev *et al.* 1988). The jets collide forming a turbulent cloud. In a stratified fluid gravity suppresses vertical motions. As a result, two dipoles form and emerge from the cloud in directions perpendicular to the initial directions of the jets. The subsequent motion of the dipoles depends on the ratio of jet intensities. If the intensities are equal, the dipoles move in a straight line. If the intensities are not equal the dipoles describe a loop and collide again. Increasing the distance between the nozzles, van Heijst & Flor (1989*a*, *b*) reproduced and described in detail a situation in which two dipoles were formed by the jets before the collision. The subsequent collision also demonstrated the emergence of unsteady vortex quadrupole. Both sets of authors confined themselves to a description of the visual observations and did not propose any theoretical explanation of the experimental observations.

A dipole impinging normally on a vertical barrier in a stratified fluid was reproduced experimentally and described in detail by van Heijst & Flor (1989*b*). Based on this experiment, Orlandi (1990) made two-dimensional numerical simulations of the collision of a dipole with a boundary. Non-slip and free-slip conditions on the boundary were discussed. The results of these numerical simulations demonstrated quite good agreement with the experiments and revealed a rather complex sequence of multiple rebounds and impingements at the intermediate stage of collision. Though the number of intermediate bifurcations increased with the Reynolds number of the flow, the final asymptotic state of the flow appeared to be very simple: two vortices (halves of the dipole) that moved apart along the wall and increased in size by viscous diffusion.

It is clear now that the results of these studies are useful in elucidating the nature and dynamics of the mushroom-like currents in the ocean. Vortex dipole interactions of different kinds cause the emergence of more complex flows. Up to now, only a few of these have been reproduced experimentally. To fill this gap we have reproduced some other types of dipole interactions in a stratified fluid and present below the experimental results obtained. Basing our work on a general theory proposed recently by Cantwell (1986), which permits us to consider, from one point of view,

different flows induced by the action of localized forces in a viscous fluid, we propose a model for two-dimensional vortex-dipole interactions and interpret the experimental results. To make the discussion of the experimental observations more constructive we postpone the experimental part of our study and consider first a theoretical model.

This paper is organized as follows. In §2 we present a theoretical analysis which permits us to connect the forces applied on a viscous fluid with appropriate vorticity distributions and introduce governing parameters for the induced two-dimensional flow, then we consider exact solutions of the two-dimensional Stokes equations for the flows induced by two equal forces directed towards one another and acting impulsively or with constant intensity: a model of the collision of two dipoles and the subsequent generation of an unsteady vortex quadrupole. In §3 we describe briefly the experimental technique used. In §4 the experimental results for different kinds of vortex dipole interactions are presented and, on the basis of the relevant parameters governing the flow, some cases of particular interest are discussed. Conclusions are given in §5.

2. Theoretical analysis

Following the paper by Cantwell (1986) consider the planar unsteady flow of a viscous incompressible fluid induced by a system of forces $\boldsymbol{F}(\boldsymbol{x}', t)$ (force per unit volume), which acts on the fluid inside the area $S'(\boldsymbol{x}')$ (figure 2). The forces and associated vorticity distribution $\boldsymbol{\omega}(\boldsymbol{x}', t) = (0, 0, \omega) = \boldsymbol{k}\omega$ are assumed to occupy a finite area $S'(\boldsymbol{x}')$ and the fluid extends to infinity ($\boldsymbol{k}$ being the unit vector along z-axis perpendicular to the plane of motion). The vector potential $\boldsymbol{B}(\boldsymbol{x}, t) = (0, 0, \psi) = \boldsymbol{k}\psi$, where $\psi(\boldsymbol{x}, t)$ is the stream function at a point $\boldsymbol{x}$, can be found from the vector Poisson equation

$$\nabla^2 \boldsymbol{B} = -\boldsymbol{\omega}, \tag{2.1}$$

the solution of which for two dimensions is

$$\boldsymbol{B}(\boldsymbol{x}, t) = -\frac{1}{2\pi}\int_{S'} \boldsymbol{\omega}(\boldsymbol{x}', t) \ln|\boldsymbol{x} - \boldsymbol{x}'| \, \mathrm{d}S'. \tag{2.2}$$

2.1. *Multipole expansion and governing equations*

For $|\boldsymbol{x}| \gg |\boldsymbol{x}'|$ the vector potential (2.2) may be approximated by a few terms of a multipole expansion

$$\boldsymbol{B} = \boldsymbol{k}\left[-\frac{\ln|\boldsymbol{x}|}{2\pi}\Gamma + \frac{n_i}{2\pi|\boldsymbol{x}|}D_i + \frac{n_i n_j}{4\pi|\boldsymbol{x}|^2}Q_{ij} + O\left(\frac{1}{|\boldsymbol{x}|^3}\right)\right], \tag{2.3}$$

where

$$\Gamma = \int_{S'} \omega(\boldsymbol{x}', t) \, \mathrm{d}S', \tag{2.4}$$

$$D_i = \int_{S'} \boldsymbol{x}_i' \, \omega(\boldsymbol{x}', t) \, \mathrm{d}S', \tag{2.5}$$

$$Q_{ij} = \int_{S'} (2\boldsymbol{x}_i' \boldsymbol{x}_j' - (\boldsymbol{x}')^2 \delta_{ij}) \, \omega(\boldsymbol{x}', t) \, \mathrm{d}S' \tag{2.6}$$

and $n_i = x_i/|\boldsymbol{x}|$, $\boldsymbol{x} = (x_1, x_2)$. In addition to the monopolar term (2.4) and dipolar term (2.5), the case considered by Cantwell (1986), the third quadrupolar term (2.6) is added in expansion (2.3).

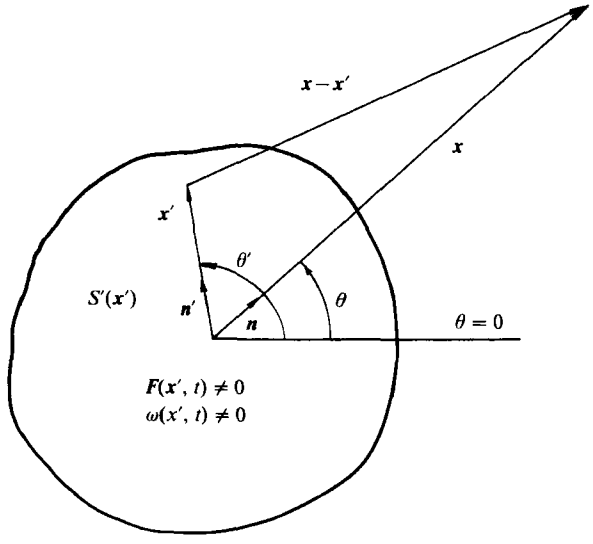

FIGURE 2. Sketch of the flow and coordinate system.

The fact that ω is divergence free and localized and forces apply no net moment to the fluid implies that $\Gamma = 0$. After some algebra the multipole expansion (2.3) in a polar coordinate system (r, θ) can be presented in the form

$$\psi(r,\theta,t) = \frac{1}{2\pi r}\int_0^{2\pi}\int_0^{\infty} \cos(\theta-\theta')\,\omega(r',\theta',t)\,(r')^2\,\mathrm{d}r'\,\mathrm{d}\theta' + \frac{1}{4\pi r^2}\int_0^{2\pi}\int_0^{\infty} \cos 2(\theta-\theta')\,\omega(r',\theta',t)\,(r')^3\,\mathrm{d}r'\,\mathrm{d}\theta' + O\left(\frac{1}{r^3}\right). \quad (2.7)$$

The full nonlinear problem is too complicated for analysis, thus consider Stokes' equation for vorticity

$$r^2\omega_t = \nu(\omega_{\theta\theta} + r\omega_r + r^2\omega_{rr}). \quad (2.8)$$

Taking into account the expansion (2.7), we are looking for self-similar solutions of (2.8) in the form (Barenblatt *et al.* 1989)

$$\omega = At^m W(\xi)\cos[n(\theta+\theta_0)], \quad \xi = \frac{r}{2(\nu t)^{\frac{1}{2}}}, \quad (2.9)$$

where ν is the viscosity, A, m, θ_0 are constants, and $n = 1, 2, \ldots$. From (2.8) for $W(\xi)$ we obtain the governing ordinary differential equation

$$\frac{\mathrm{d}^2W}{\mathrm{d}\xi^2} + (2\xi + \xi^{-1})\frac{\mathrm{d}W}{\mathrm{d}\xi} - (n\xi^{-2} + 4m)\,W = 0. \quad (2.10)$$

A general solution of (2.10) can be expressed via the confluent hypergeometric functions (see e.g. Kamke 1959). The stream function can be found from the equation

$$\psi_{\theta\theta} + r\psi_r + r^2\psi_{rr} = -r^2\omega. \quad (2.11)$$

Consider now some cases of practical interest.

2.2. *Vortex dipole*

Consider a flow induced by a point momentum source which acts impulsively at time $t = 0$ and exerts on the fluid a force

$$J\rho = \int_{S'} F \, \mathrm{d}S' = I\rho\,\delta(t)$$

in the direction $\theta = 0$ in a polar coordinate system (r, θ) ($\delta(t)$ is the delta function, ρ is the fluid density). The source is at the point $r = 0$. The dimensions of I are L^3T^{-1} and $I = \text{const}$.

On dimensional grounds and from the geometry we have:

$$A = I/\nu^{\frac{3}{2}},\ m = -\tfrac{3}{2},\ \theta_0 = \tfrac{1}{2}\pi,\ n = 1.$$

For these m and n, the solution of (2.10) that is non-singular at $\xi = 0$ for $t > 0$ and satisfies the condition $W(\xi) \to 0$ when $\xi \to \infty$ is

$$W(\xi) = C\xi \exp(-\xi^2). \tag{2.12}$$

The fact that the impulse of the vorticity distribution (first integral in (2.7)) is equal to the total impulse, $I = \int_0^t J \, \mathrm{d}t$, applied by the force distribution since the onset of the motion (Cantwell 1986), where

$$I(t) = \int_0^{2\pi} \int_0^{\infty} \sin\theta' \omega(r', \theta', t) (r')^2 \, \mathrm{d}r' \, \mathrm{d}\theta', \tag{2.13}$$

gives $C = 1/(4\pi)$ in (2.12). Thus for the vorticity we have

$$\omega = \frac{Ir}{8\pi(\nu t)^2} \exp(-r^2/4\nu t) \sin\theta. \tag{2.14}$$

Solving (2.11) for the stream function we obtain

$$\psi = \frac{I}{2\pi r}(1 - \exp(-r^2/4\nu t)) \sin\theta. \tag{2.15}$$

Consider now the case in which a point momentum source acts continuously: it starts at time $t = 0$ and thereafter exerts on the fluid a force $J\rho$ in the direction $\theta = 0$. The dimensions of J are L^3T^{-2} and $J = \text{const}$. Using the same arguments as above (for this case $A = J/\nu^{\frac{3}{2}}$, $m = -\frac{1}{2}$, $\theta_0 = \frac{1}{2}\pi$, $n = 1$) we obtain

$$\omega = \frac{J}{2\pi\nu r} \exp(-r^2/4\nu t) \sin\theta, \tag{2.16}$$

$$\psi = \frac{Jr}{2\pi\nu}\left[\frac{\nu t}{r^2}(1 - \exp(-r^2/4\nu t)) + \frac{1}{4}\int_{r^2/4\nu t}^{\infty} \mathrm{e}^{-x} x^{-1} \, \mathrm{d}x\right] \sin\theta. \tag{2.17}$$

Integrating the equations of motion for marked particles

$$\frac{\mathrm{d}r}{\mathrm{d}t} = \frac{1}{r}\psi_\theta, \quad \frac{\mathrm{d}\theta}{\mathrm{d}t} = -\frac{1}{r}\psi_r \tag{2.18}$$

with the stream function (2.17) or (2.15), one can calculate the distributions of the marked particles and compare them with the dyed water distributions in a real flow. The results of comparisons with the visualized flows induced in a linearly stratified

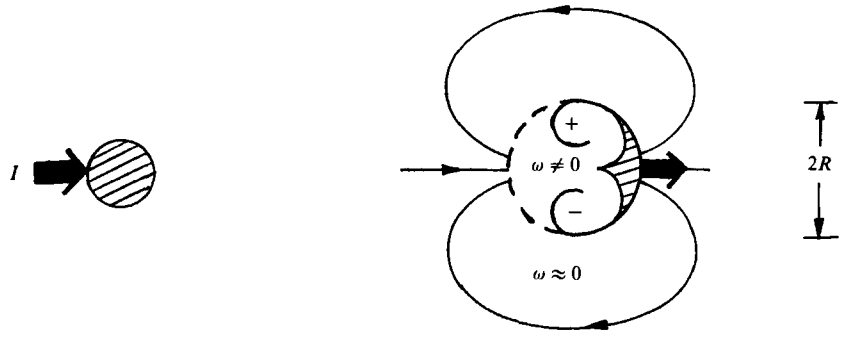

FIGURE 3. Sketch of dipole formation under the action of a localized force: appropriate dyed water distributions (shaded area), vortical flow ($\omega \neq 0$), potential flow ($\omega = 0$).

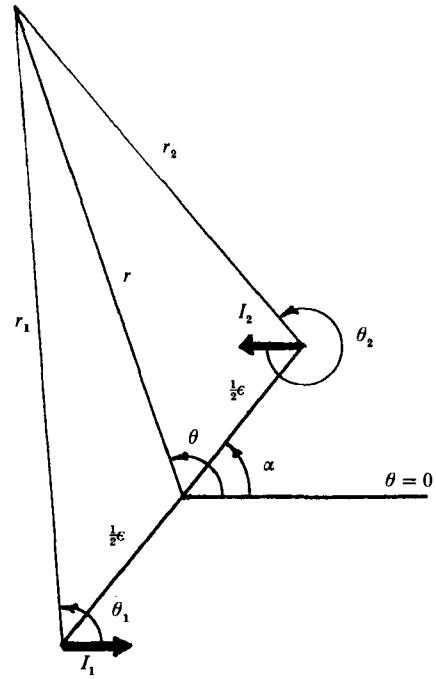

FIGURE 4. Sketch of two equal ($I_1 = I_2 = I$) forces acting on fluid in opposite directions: $\theta = \pi$, $\theta = 0$, α is an arbitrary angle.

fluid (Afanasyev & Voropayev 1989*b*) and in a two-layer fluid (Voropayev *et al.* 1991) have demonstrated that the model correctly reproduces the gross features of the real dipole generated by a localized force in a viscous fluid. Dipole formation, and the appropriate distributions of dyed fluid, vortical and potential flows are shown schematically in figure 3.

2.3. *Vortex quadrupole*

Consider two point sources of momentum exerting on the fluid equal forces $J\rho$ in opposite directions (figure 4). The sources are at the points $(\frac{1}{2}\epsilon, \alpha)$, $(\frac{1}{2}\epsilon, \alpha + \pi)$ and act on the fluid in the directions $\theta = \pi$, $\theta = 0$ respectively (α is an arbitrary angle).

Decreasing ϵ and increasing J so that the product $\epsilon J = M$ remains constant, we obtain a point source of intensity $M\rho$ at the point $r = 0$. The source consisting of two forces (figure 4) is a force dipole for $\alpha = 0, \pi$ and a pair of forces for $\alpha = \pm\frac{1}{2}\pi$. For arbitrary α we have a combination of the two types of sources. The force dipole applies no net force on the fluid hence the dipolar distribution (2.13) is equal to zero and the first non-zero term in (2.7) is the term with quadrupolar distribution (second integral in (2.7)), hence $\omega \sim \cos 2(\theta+\theta_0)$.

Consider again two cases: an impulsive source and a source of constant intensity. In the first case $M = Q\delta(t)$. The dimensions of Q are L^4T^{-1} and $Q = \text{const}$. Hence in (2.9) $A = Q/\nu^2$, $m = -2$, $n = 2$ and from (2.10) we obtain the solution

$$W(\xi) = C\xi^2 \exp(-\xi^2). \tag{2.19}$$

For the source of constant intensity $M\rho$ which starts at $t = 0$ the dimensions of M are L^4T^{-2} and $M = \text{const}$. Hence $A = M/\nu^2$, $m = -1$, $n = 2$ in (2.9) and from (2.10) we obtain the solution

$$W(\xi) = C(1+\xi^{-2}) \exp(-\xi^2). \tag{2.20}$$

To determine a constant of integration C in (2.19) and (2.20) we need the connection (similar to (2.13) between the source intensity and appropriate quadrupolar vorticity distribution. Besides that we must find some additional arguments to determine a constant θ_0 in (2.9).

For large r the stream function (2.15) or (2.17) for the flow induced by a point force is

$$\psi_0 = \frac{I}{2\pi r}\sin\theta, \tag{2.21}$$

where $I = \text{const}$ for an impulsive force and $I = Jt$ for a constant force ($J = \text{const}$). Representing the stream function for two equal forces ($I_1 = I_2 = I$) shown in figure 4 as the superposition of stream functions (2.21), for large r we have

$$\psi = \frac{I}{2\pi}\left(\frac{\sin\theta_1}{r_1} + \frac{\sin\theta_2}{r_2}\right). \tag{2.22}$$

From the geometry (see figure 4) we have

$$\begin{aligned} r_1^2 &= r^2 + (\tfrac{1}{2}\epsilon)^2 + \epsilon r\cos(\theta-\alpha), \\ r_2^2 &= r^2 + (\tfrac{1}{2}\epsilon)^2 - \epsilon r\cos(\theta-\alpha), \\ r_1\sin\theta_1 &= r\sin\theta + (\tfrac{1}{2}\epsilon)\sin\alpha, \\ r_2\sin\theta_2 &= -r\sin\theta + (\tfrac{1}{2}\epsilon)\sin\alpha, \end{aligned}$$

and for $r \gg \frac{1}{2}\epsilon$ with an accuracy of order $\epsilon/2r$ for the force dipole we obtain

$$\psi = -\frac{Q}{2\pi r^2}\sin(2\theta-\alpha), \tag{2.23}$$

where $Q = \epsilon I$.

Comparing (2.23) with the second term in expansion (2.7) we obtain the condition determining the constants C and θ_0:

$$-Q\sin(2\theta-\alpha) = \frac{1}{2}\int_0^{2\pi}\int_0^{\infty} \cos 2(\theta-\theta')\,\omega(r',\theta',t)\,(r')^3\,\mathrm{d}r'\,\mathrm{d}\theta'. \tag{2.24}$$

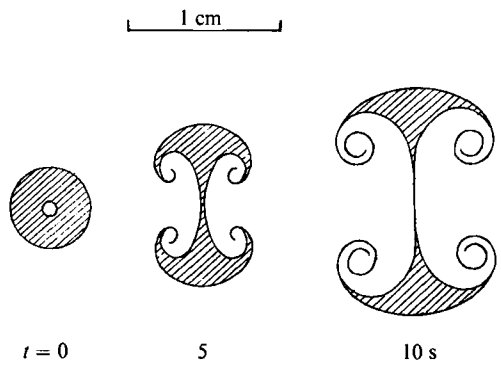

FIGURE 5. Dyed water distribution (shaded area) in a planar impulsive vortex quadrupole calculated with the stream function (2.26). The contours of shaded area were obtained by calculations of the trajectories of 10 marked particles in the first quadrant. The final positions of the particles for different times were drawn by hand. To avoid the singularity, particles which had initial positions near the point $r = 0$ were not considered. $Q = 2$ cm^4 s^{-1}, $\nu = 10^{-2}$ cm^2 s^{-1}.

Using this condition after some algebra we find: $C = 1/(8\pi)$, $\theta_0 = -\frac{1}{2}\alpha - \frac{1}{4}\pi$. Inserting these constants into (2.19), (2.20) and (2.9) and solving (2.11) we obtain two solutions. For the impulsive source:

$$\omega = -\frac{Qr^2}{32\pi\nu^3 t^3}\exp(-r^2/4\nu t)\sin(2\theta-\alpha), \tag{2.25}$$

$$\psi = -\frac{Q}{2\pi r^2}\left[1-\left(1+\frac{r^2}{4\nu t}\right)\exp(-r^2/4\nu t)\right]\sin(2\theta-\alpha). \tag{2.26}$$

For the source of constant intensity ($Q = Mt$, $M = \text{const}$):

$$\omega = -\frac{M}{8\pi\nu^2 t}\left(1+\frac{4\nu t}{r^2}\right)\exp(-r^2/4\nu t)\sin(2\theta-\alpha), \tag{2.27}$$

$$\psi = -\frac{Mt}{2\pi r^2}(1-\exp(-r^2/4\nu t)\sin(2\theta-\alpha). \tag{2.28}$$

Integrating the equations of motion (2.18) with the stream function (2.26) or (2.28) one can calculate the distributions of marked particles which initially were in a small circle around the source ($r = 0$). These distributions are shown for the impulsive force dipole (2.26) in figure 5. Thus two equal forces acting in opposite directions induce the vortex quadrupole consisting of two dipoles moving in the directions $\theta = \frac{1}{2}(\alpha \pm \pi)$. Vortex quadrupole formation and appropriate distributions of dyed fluid, vortical and potential flows are shown schematically in figure 6.

Thus the action of a single force or of the simplest system of forces (two equal forces) on a viscous fluid leads to the formation of a compact vortex dipole or a quadrupole, respectively. The governing parameter for the dipole is the integral intensity (I) of the dipolar vorticity distribution (momentum of the dipole). Correspondingly, for the quadrupole it is the integral intensity (Q) of the quadrupole vorticity distribution. I and Q are determined by the intensity of the initial force action on the fluid. Note, that vorticity in these vortex structures is localized in a compact fluid volume of radius R (figure 3). The following interpretation of experimental results is based on the idea of vortex multipoles governed by the parameters introduced above.

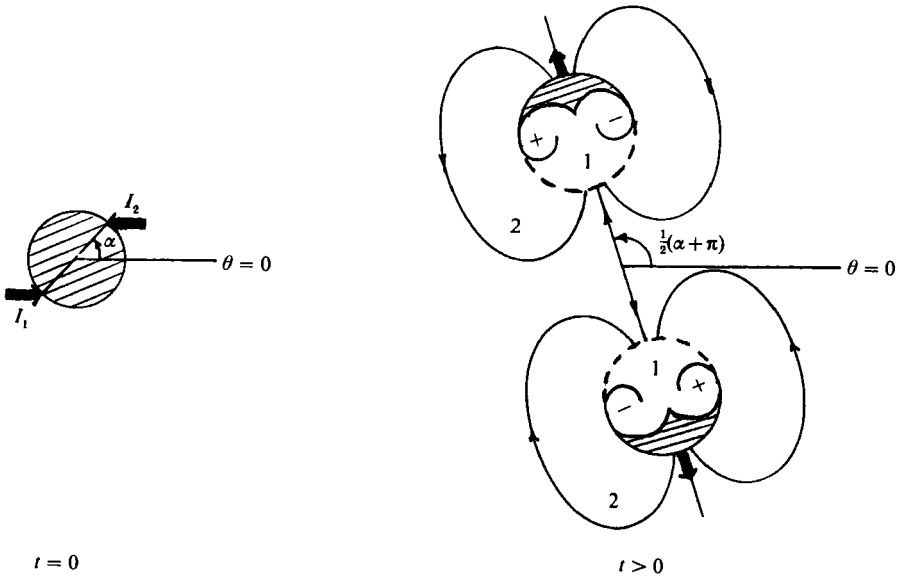

FIGURE 6. Sketch of quadrupole formation under the action of two equal forces of opposite direction: appropriate dyed water distributions (shaded area), (1) vortical flow, (2) potential flow.

3. Description of the experiment

The technique used for the generation of vortex dipoles in the experiments discussed in this paper is similar to those described in detail in other papers concerning this subject (Voropayev & Filippov 1985; Voropayev *et al.* 1991). Here we omit the details and present only a brief description of the experimental set-up.

The experiments were performed in a transparent Plexiglas tank, of rectangular shape, $80 \times 80 \times 30$ cm. A density stratification in the working fluid (distilled water) was created by varying its salinity in the vertical direction. A strong, linear, vertical density distribution with buoyancy frequency $N = 1.5\ \mathrm{s}^{-1}$ was produced using the two-tank method.

The flows in the tank were generated by horizontal jets from one or two thin round nozzles – localized sources of momentum (nozzle diameter $D = 0.1$–0.2 cm). Dyed jets were injected horizontally into the stratified fluid at the level of their equilibrium density (ρ). A jet exerts on the fluid a localized force $j = 4\rho q^2/(\pi D^2)$ and imparts to the fluid a localized impulse given by $i = \int_0^t j\,\mathrm{d}t$ (q is the measured volume flux from the nozzle). The dimensions of j for a round source are L^4T^{-2}. To characterize the source intensity we shall use a non-dimensional parameter j/ν^2 which is almost equal to a squared Reynolds number (Re) of the jet flow generated by the source: $j/\nu^2 \approx Re$ (e.g. see Batchelor 1967). For an impulsive source the flow momentum $i = j\,\Delta t = \mathrm{const}$, where Δt is the duration of the action of the force. Its typical value in our experiments is $\Delta t \approx 3$–5 s. For a source of constant intensity, the flow momentum, $i = jt$, increases with time.

The results of previous experiments and theoretical analysis demonstrate that the Richardson number of a vortex dipole, generated by localized force action in a stratified fluid, rapidly increases with time. Thus the flow at the intermediate-asymptotic stage can be considered as an approximately two-dimensional one, the vertical lengthscale (H) of the dipole being determined by the initial Reynolds

number of the flow and a stratification parameter (Voropayev *et al.* 1991). The model presented in the latter paper permits one to calculate the main vortex-dipole characteristics (including H). Thus, in our further qualitative analysis we consider the dipoles as planar and characterize their intensity in terms of momentum per unit depth $I = i/H$. Applying the same arguments for a quadrupole, we also obtain the quadrupole intensity in the form $Q = I\epsilon = \epsilon i/H$. For the horizontal lengthscale of the flow, we use the typical lengthscale (R) of the dyed water region and take into account that R increases with time. The values of the initial Reynolds number (Re) for each case are given in the figure captions. The buoyancy frequency in all experiments was $N \approx 1.5\ \mathrm{s}^{-1}$.

In the experiments in which we studied the interaction of a dipole with a wall, we used a glass plate which was placed vertically in the tank.

The flows were visualized by adding a pH-indicator, thymol blue dye, to the working fluid (Stern & Voropayev 1984). The fluid in the tank was acidic (yellow). The fluid injected from the nozzle was in the basic form (blue) so the flow was clearly visible. After the end of each test we waited several minutes until the injected (blue) fluid in the tank became yellow again by a diffusive chemical reaction with the acidic surroundings. Thus we could perform the next experiment without changing the working fluid in the tank.

4. Experimental results and interpretation

In this section we present results from experiments documenting the dynamics of vortex-dipole interactions. Some representative photographic sequences are given in the figures in this section. We also present a qualitative interpretation of the experimental results in terms of forces acting on the fluid and associated vortex multipoles: dipoles, quadrupoles and their combinations.

4.1. *Head-on collision of two dipoles of equal momenta*

Consider two sources of momentum which start simultaneously and thereafter apply to the fluid equal forces, acting in opposite directions for a time Δt. After the onset, the sources generate two initially turbulent strong jets ($Re \approx 700$, figure 7*a*). The jets, which have equal momenta ($I_1 = I_2 = I$), collide, forming a chaotic, turbulent, three-dimensional cloud (figure 7*b*). Owing to gravity, the flow becomes quasi-planar. As a result of the collision, two dipoles are pushed from the cloud in opposite directions, perpendicular to the initial directions of motion of the jets (figures 7*c* and 7*d*). A similar kind of collision was also observed by van Heijst & Flor (1989*a*) with the only difference that, in their experiment, primary dipoles were formed from the jets before the collision.

Consider now the same interaction but for laminar flows ($Re \approx 45$, figure 8). The initial jets are weak and the flow is laminar from the start; thus the jets form two dipoles before the collision (figure 8*a*). These dipoles move towards one another forming a quadrupole (figure 8*b*) consisting of the vortices of the primary dipoles. Two newly formed dipoles then move apart perpendicular to the initial directions of motion of the primary dipoles (figure 8*c*, *d*). Of course, the initial flows in figures 7(*a*) and 8(*a*) look very different but the final result of the interactions (figures 7*d* and 8*d*), i.e. the formation of dipoles of equal intensity moving apart, is the same for both cases. It is clear that, at least qualitatively, we can consider the interaction dynamics without emphasizing the regime of the flow (whether it is turbulent or laminar initially) and below we present only the most informative examples.

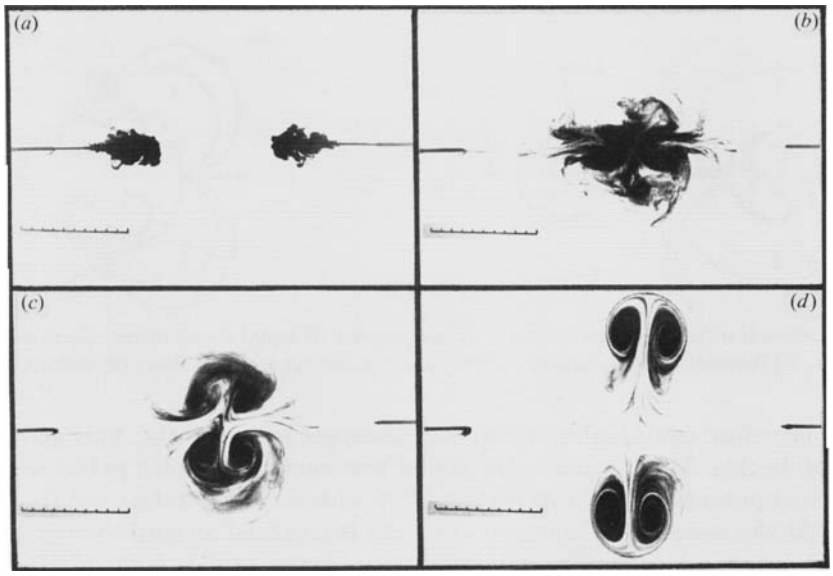

FIGURE 7 (*a–d*). Photographic sequence showing a top view of the collision of two impulsive strong jets ($Re \approx 700$) of equal momentum and the formation of an impulsive vortex quadrupole in a linearly stratified ($N = 1.5\ \mathrm{s}^{-1}$) fluid. Scale in cm. Distance between the sources $\epsilon = 15$ cm.

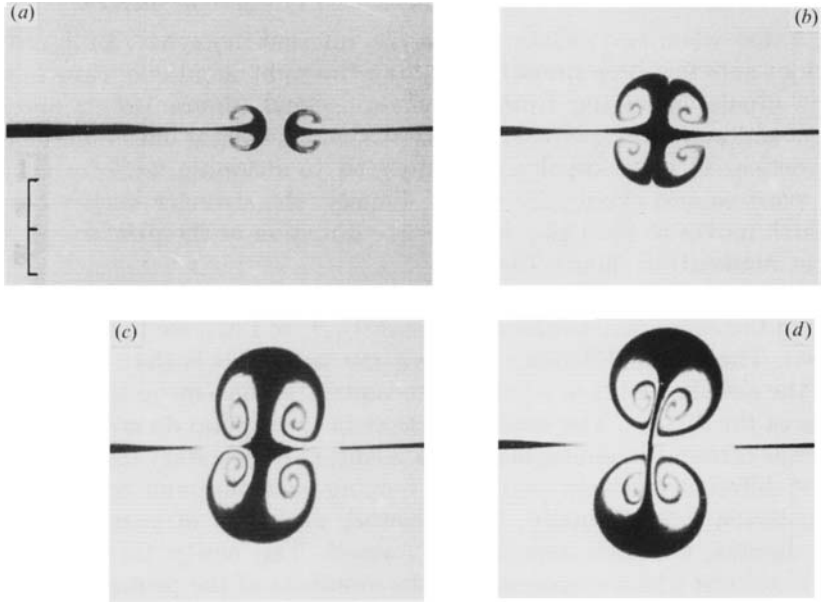

FIGURE 8 (*a–d*). Photographic sequence showing the head-on collision of two dipoles ($Re \approx 45$) of equal momentum and the formation of a vortex quadrupole. Scale in cm. Distance between the sources $\epsilon = 2.5$ cm. (*a*) $t = 2$ s, (*b*) 7 s, (*c*) 13 s, (*d*) 19 s.

Consider now the same interaction in terms of vortex multipoles. For this case the total momentum of the flow is equal to zero, hence we have only one parameter – the quadrupolar intensity of the flow $Q = I\epsilon$, where ϵ is the distance between the two sources. After the sources start, two primary dipoles form. Initially ($R < \frac{1}{2}\epsilon$) they develop independently, governed by the parameters I_1, I_2 ($I_1 = I_2$) respectively (figure 8*a*). When the dipole radius R, which is also a lengthscale of the vortical

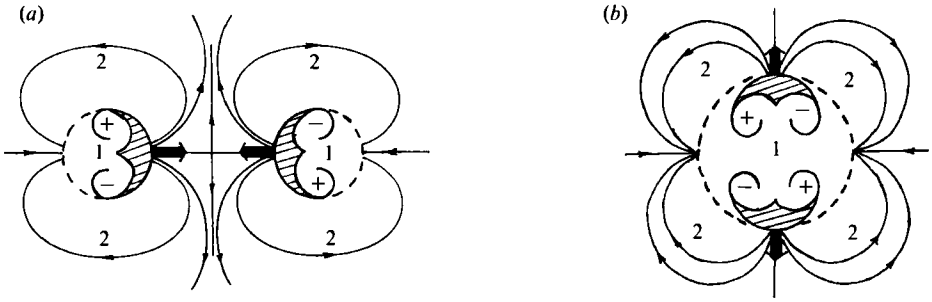

FIGURE 9. Sketch of the head-on collision of two dipoles of equal momentum: (*a*) initial phase of interaction, (*b*) formation of compact vortex quadrupole; (1) vortical flow, (2) potential flow.

patches, becomes comparable with the distance between the two patches, the interaction begins. The mutual induction of two vortical, dipolar patches causes the emergence of potential, quadrupolar backflow outside the patches (see the sketch in figure 9). At the moment of collision, vorticity is localized around the collision point (figure 8*b*). Thus, a localized vortex quadrupole forms at this point (figure 9*b*). The subsequent flow evolution is governed by the single parameter Q. As a consequence, the quadrupole flow develops in accordance to the theoretical solution (2.26) shown in figure 5.

4.2. *Head-on collision of two dipoles of different momenta*

Consider a case when two colliding jets have different momenta. In figure 10(*a*) the left-hand jet acts for three times longer than the right-hand one, thus $I_1 = 3I_2$. The secondary dipoles emerging from the chaotic cloud (figure 10*b*, *c*) are no longer symmetric and move along circular paths instead of straight lines (figure 10*c*–*e*). The weaker vortices in these dipoles are subjected to straining while orbiting around stronger vortices and eventually decay. Finally, the stronger vortices form a new dipole which moves to the right, in the same direction as the primary jet which has the largest momentum (figure 10*e*, *f*).

It is interesting to compare the case considered ($I_1 = 3I_2$) with one when the momenta of the colliding jets differ only slightly ($I_1 \approx 1.3I_2$, see figure 4 in Afanasyev *et al.* 1988). The major difference between the two cases is that, in the latter, the radius of the circular paths in which the secondary dipoles move is much larger than the radius of the dipoles. The weaker vortices in the dipoles do not decay in the less intensive background straining field. As a result, two secondary dipoles consisting of vortices of different intensity perform a looping excursion and collide again at the original collision point. Finally, after another exchange of partners between the colliding dipoles, two new dipoles are formed. The newly formed dipoles have different momenta which correspond to the momenta of the primary jets. Note that the common radius of the circular paths in which the secondary dipoles move depends on the ratio I_1/I_2. When $I_1/I_2 \to 1$ this radius tends to infinity and we have a 'pure' quadrupole (§4.1).

Consider the collision shown in figure 10 in terms of its governing parameters. For this case, both of the parameters $I = I_1 - I_2$ and $Q = I_2\epsilon$ are non-zero. The summary flow can be considered as a superposition of dipolar (I) and quadrupolar (Q) flows. The velocities induced by a dipole and a quadrupole decrease with distance as r^{-2} and r^{-3} respectively (see §2). Thus at small distances a quadrupolar flow prevails. As a result, two secondary dipoles governed by the parameter Q emerge from the cloud after the collision (figure 10*b*, *c*). At larger distances dipolar flow prevails. As a result, the

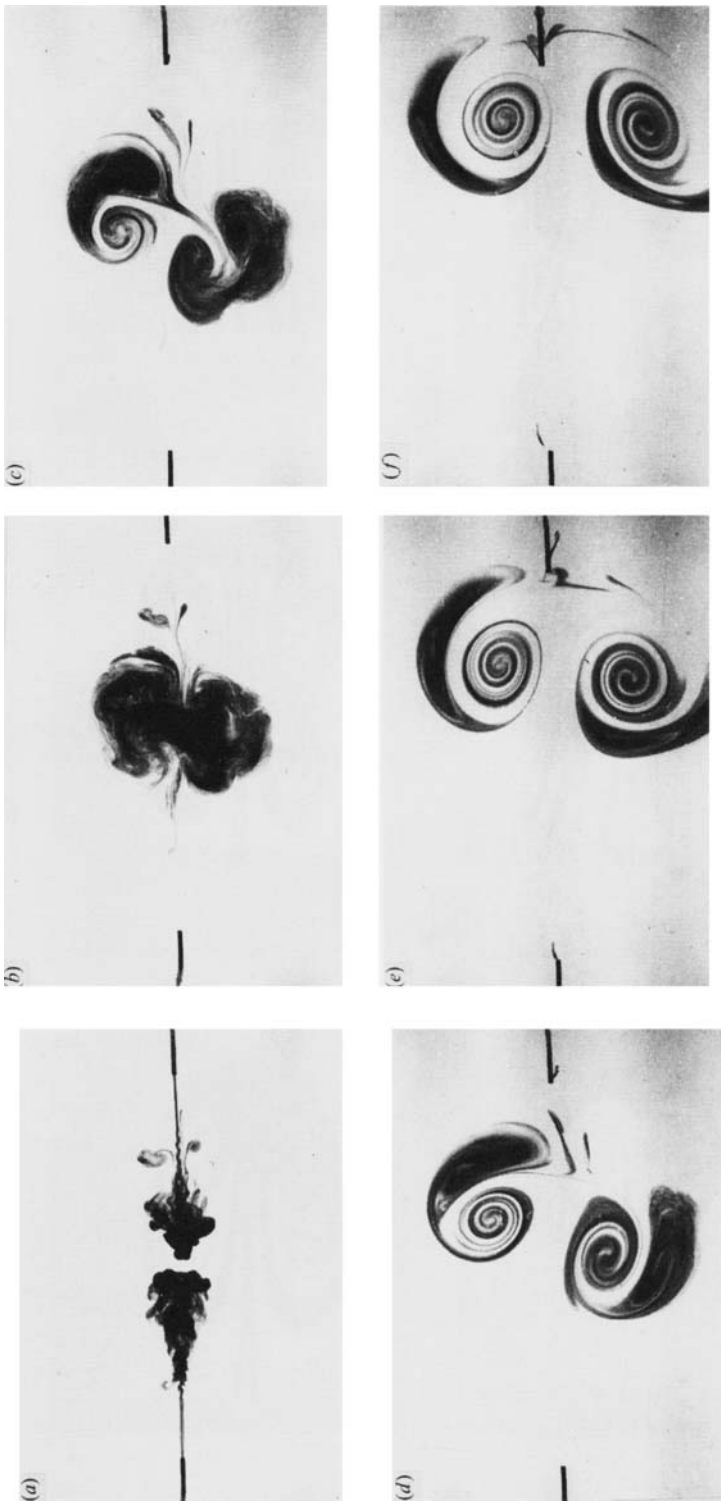

FIGURE 10(*a–f*). Photographic sequence showing the collision of two impulsive strong jets ($Re \approx 700$) of different momentum : two sources of equal intensity act for periods of time 6 s and 2 s respectively, thus the left-hand source applies to the fluid a total momentum which is three times greater than that applied by the right-hand source. Distance between the sources $\epsilon = 14.5$ cm.

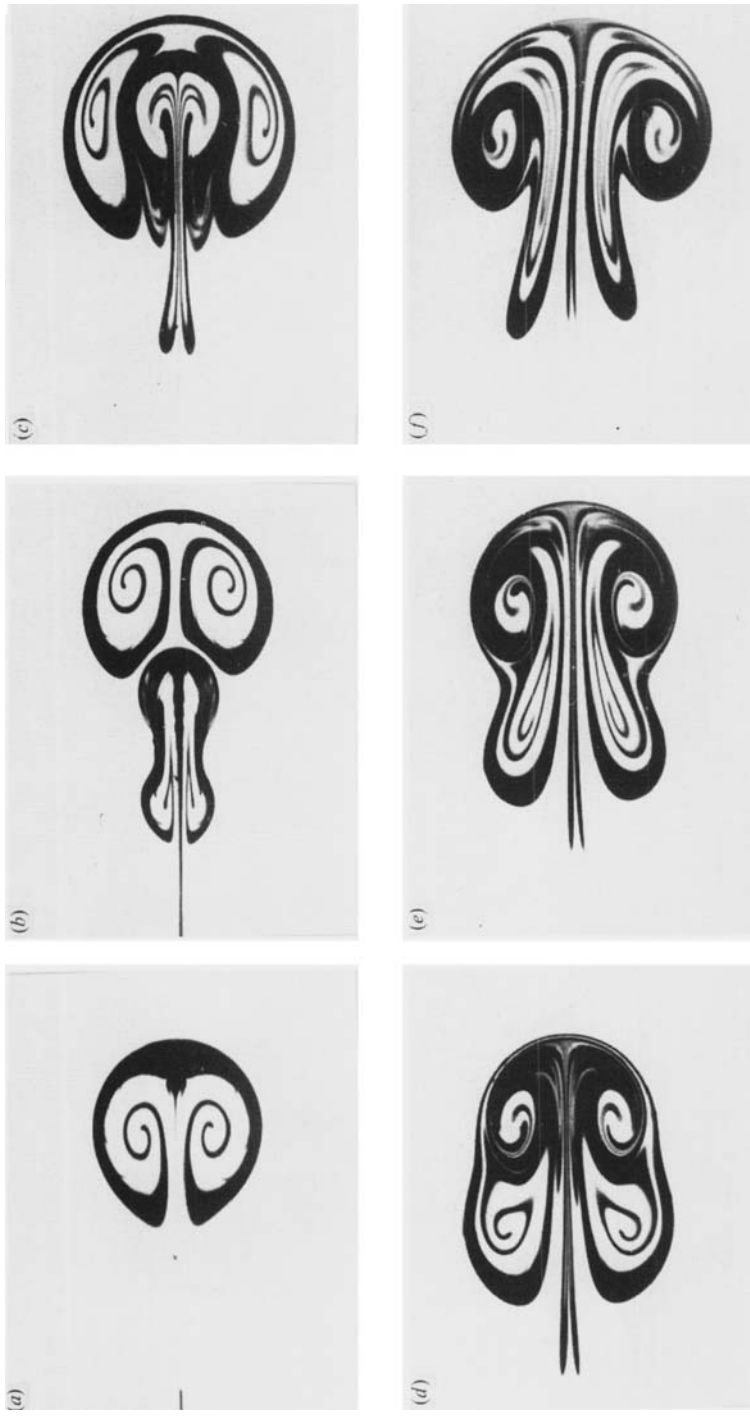

FIGURE 11 (*a–f*). Photographic sequence showing the interaction of two dipoles ($Re \approx 80$) moving one behind the other.

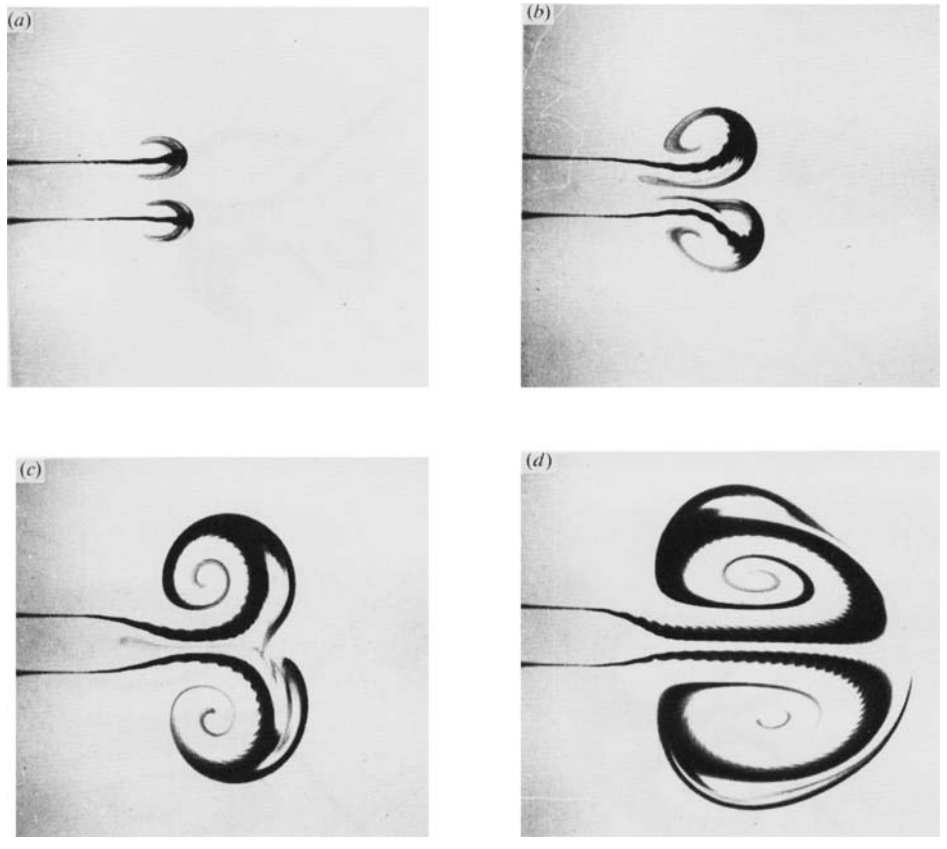

FIGURE 12 (*a–d*). Photographic sequence showing the interaction of two dipoles ($Re \approx 70$) moving in parallel. Distance between the sources $\epsilon = 2$ cm. (*a*) $t = 5.5$ s, (*b*) 16 s, (*c*) 60 s, (*d*) 118 s.

newly formed dipoles move in a background dipolar flow (figure 10*c–e*). Finally, the flow determined by the multipole of the lowest order (dipole) survives (figure 10*f*).

4.3. *Merging of two dipoles, one moving behind the other*

Consider two sources acting impulsively in the same direction along the line connecting the sources, or equivalently, one source which acts twice. The photographic sequence in figure 11 shows the flow evolution for this case. The second dipole can be seen to penetrate the first one from the rear, pushing aside the vortices of the first dipole (figure 11*b*, *c*). The strained outer vortices orbit around the vortices of the intruding second dipole (figure 11*c–e*). This continues until a single dipole forms as a result of vortex merger (figure 11*f*).

The explanation for this case is very simple. Initially, the dipoles develop independently governed by the parameters I_1, I_2 respectively. The mutual induction of two dipolar vortex patches generates a net dipolar flow of intensity $I = I_1 + I_2$. The vortex patches (dyed fluid) move in this background dipolar flow; the two dipoles merge and finally form one dipole of intensity I.

4.4. *Parallel motion of two dipoles*

Consider the interaction of two dipoles of equal intensity ($I_1 = I_2$) moving parallel to one another (figure 12). The dipoles were generated by the simultaneous action of two sources of equal intensity. In the initial period after the onset of the motion the

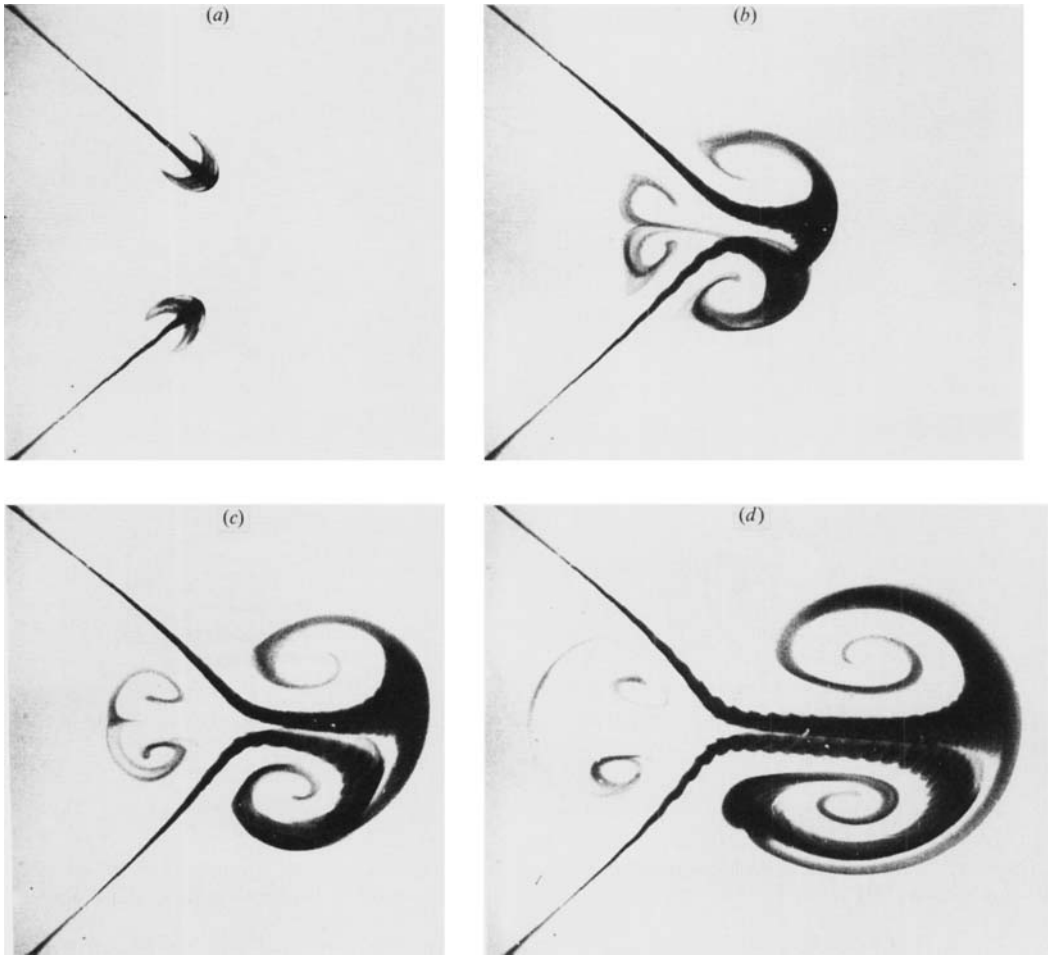

FIGURE 13(*a–d*). Photographic sequence showing the oblique collision of two dipoles ($Re \approx 60$). Distance between the sources $\epsilon = 14$ cm. (*a*) $t = 4.5$ s, (*b*) 21 s, (*c*) 32 s, (*d*) 56 s.

dipoles do not influence one another (figure 12*a*). As time progresses, the dimensions of the dipoles increase and the dipoles begin to interact. They push sideways and their inner vortices begin to orbit around the outer ones (figures 12*b*, *c*). During this process the strained (initially inner) vortices decay. The remaining vortices form the new dipole which continues to move forward (figure 12*d*).

The interpretation for this case is similar to that for the previous case. Initially, when $R < \frac{1}{2}\epsilon$ (ϵ being the distance between the sources), two primary dipoles develop independently and are clearly seen in figure 12*a*. The mutual induction of dipoles creates a net dipolar flow of intensity $I = I_1 + I_2$. The dipoles moving in this net dipolar flow (figure 12*b*, *c*) eventually form one dipole (figure 12*d*).

4.5. *Oblique collision of two dipoles*

In a case when two dipoles of equal momenta ($I_1 = I_2$) collide at some angle, each of the primary dipoles splits into two vortices and two new dipoles form. The outer vortices form a new strong dipole which moves forward. The inner vortices form a weak dipole which moves in the opposite direction (figure 13*b–d*). Note that similar

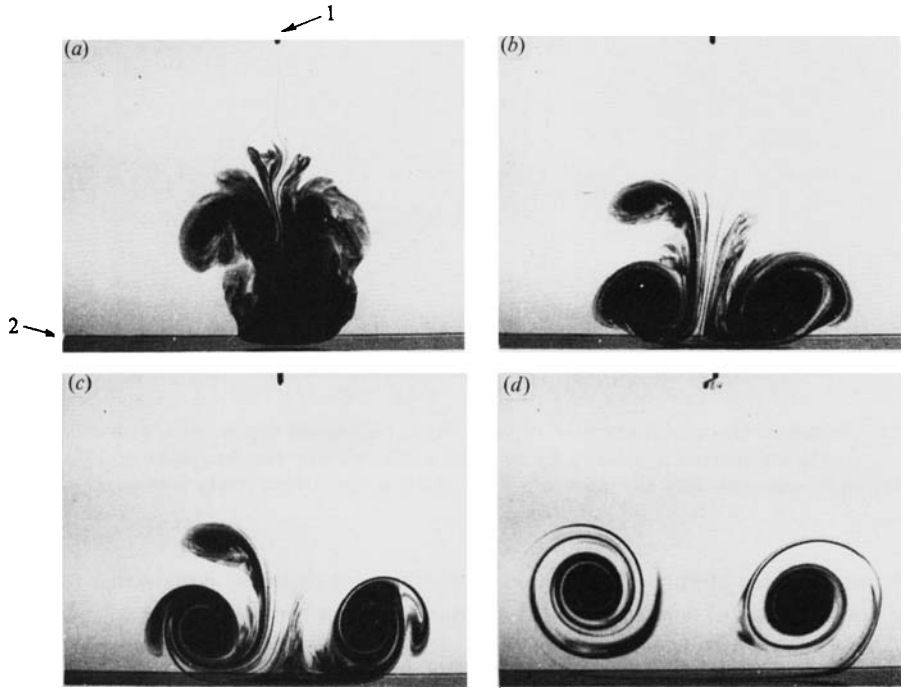

FIGURE 14 (*a–d*). Photographic sequence showing the collision of an impulsive strong jet ($Re \approx 700$) with a wall. Distance between the source (1) and the wall (2), $\epsilon = 14$ cm. (*a*) $t = 10$ s, (*b*) 51 s, (*c*) 75 s, (*d*) 136 s.

results were observed in the experiment where the quasi-two-dimensional flow was produced in a soap film (figures 12, 13 in Couder & Basdevant 1986).

The initial phase is clear: two dipoles develop independently (figure 13*a*). To explain the subsequent evolution of the flow we must take into account that the dipole intensity (momentum) is a vector. Introducing the components of the momentum vector we find that the flow shown in figure 13 is governed by two parameters: $I = 2I_1 \cos\frac{1}{2}\alpha$ and $Q = \epsilon I_1 \sin\frac{1}{2}\alpha$ (α being the angle between the directions of the sources). Thus the flow represents the superposition of dipolar and quadrupolar flows. From the geometry it is clear that the induced velocities are in the same sense to the right of the collision point, and in opposite senses on the left-hand side. The outer vortices of the primary dipoles develop in the accompanying background dipolar flow and form an intensive dipole (figure 13*b*). The inner vortices develop against the background dipolar flow forming a weak dipole (figure 13*b*) which eventually decays (figure 13*c*, *d*).

4.6. *Head-on collision of a dipole with a wall*

As mentioned above, a vortex dipole impinging on a solid wall was visualized in a recent experiment by van Heijst & Flor (1989*a*). We have reproduced a similar experiment and present some photos of the flow in figure 14.

The source of momentum of intensity I_0 is at distance ϵ from the wall and is directed normally to the wall. In contrast to the case considered by the aforementioned authors, in our experiment the source of momentum was not sufficiently far from the wall for a primary dipole to be formed before the collision. Initially, a turbulent cloud impinges on the wall (figure 14*a*) and eventually splits

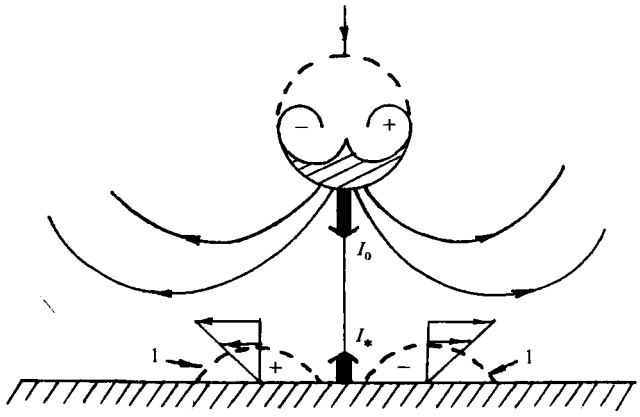

FIGURE 15. Skètch of the initial stage of the collision of a vortex dipole with a wall. Secondary vortex patches (1) are created in the boundary layer at the wall by the flow induced by the dipole. Two arrows show schematically the momenta I_0, I_* of the primary and newly formed dipolar vortex patches.

forming two dipoles (figure 14*b*). The newly formed dipoles, consisting of intense primary vortices and of weaker satellites, rebound from the wall and move in circular paths (figure 14*c*). Note that in spite of different initial conditions, the intermediate phase of flow evolution shown in figure 14*c* is very similar to the flow shown in figure 9*b* in van Heijst & Flor (1989*a*). The weaker satellites eventually decay. As a result, two large vortices of increasing radius move gradually apart along the wall.

If there was a free-slip condition at the wall, one would expect the situation to be similar to the collision of two dipoles of equal intensity (see §4.1). In that case, the wall would act only as a mirror. But in a real fluid, vorticity is created at the wall. Consequently, the flow for non-slip and for free-slip conditions is different. When the source begins to act, the induced, potential, dipolar flow causes the emergence of friction forces in the boundary layer at the wall. These forces generate two vortical patches of opposite sign (see the sketch in figure 15). These patches can be considered as a newly formed dipole directed away from the wall.

To explain the subsequent evolution of the flow, consider the interaction of primary and newly formed dipoles. This stage of the process can be interpreted in the same way as the collision of two dipoles of different intensities (§4.2). Thus, in addition to the main governing parameter – the momentum I_0 of the primary dipolar patch – we can introduce the momentum I_* of the dipolar vorticity distribution generated at the wall. We do not know the exact value of I_* which is a function of the initial governing parameters and time, but, evidently, it cannot exceed I_0. Thus two parameters govern the flow dynamics: $I = I_0 - I_*$ and $Q_* = I_* \epsilon$. Owing to the virtual quadrupole, two dipoles, consisting of vortices from the split primary dipole and vortices detached from the wall, are formed. These dipoles then move in looping curves in the net background dipolar flow of intensity I (figure 14*b*, *c*). The weaker satellites, generated at the wall, decay while orbiting around the primary vortices. As a result, a single, final dipole is formed (figure 14*d*) as if the process has returned to the beginning, with one essential difference: the momentum of the final dipole (I) is smaller than that of the primary dipole (I_0). Thus the wall reduces the momentum of the flow by this process. Consider now the effect of the image vortices on the flow dynamics. We can interpret this stage of interaction using the same arguments as for a head-on collision of two dipoles of equal intensity (§4.1). As a result, two vortices

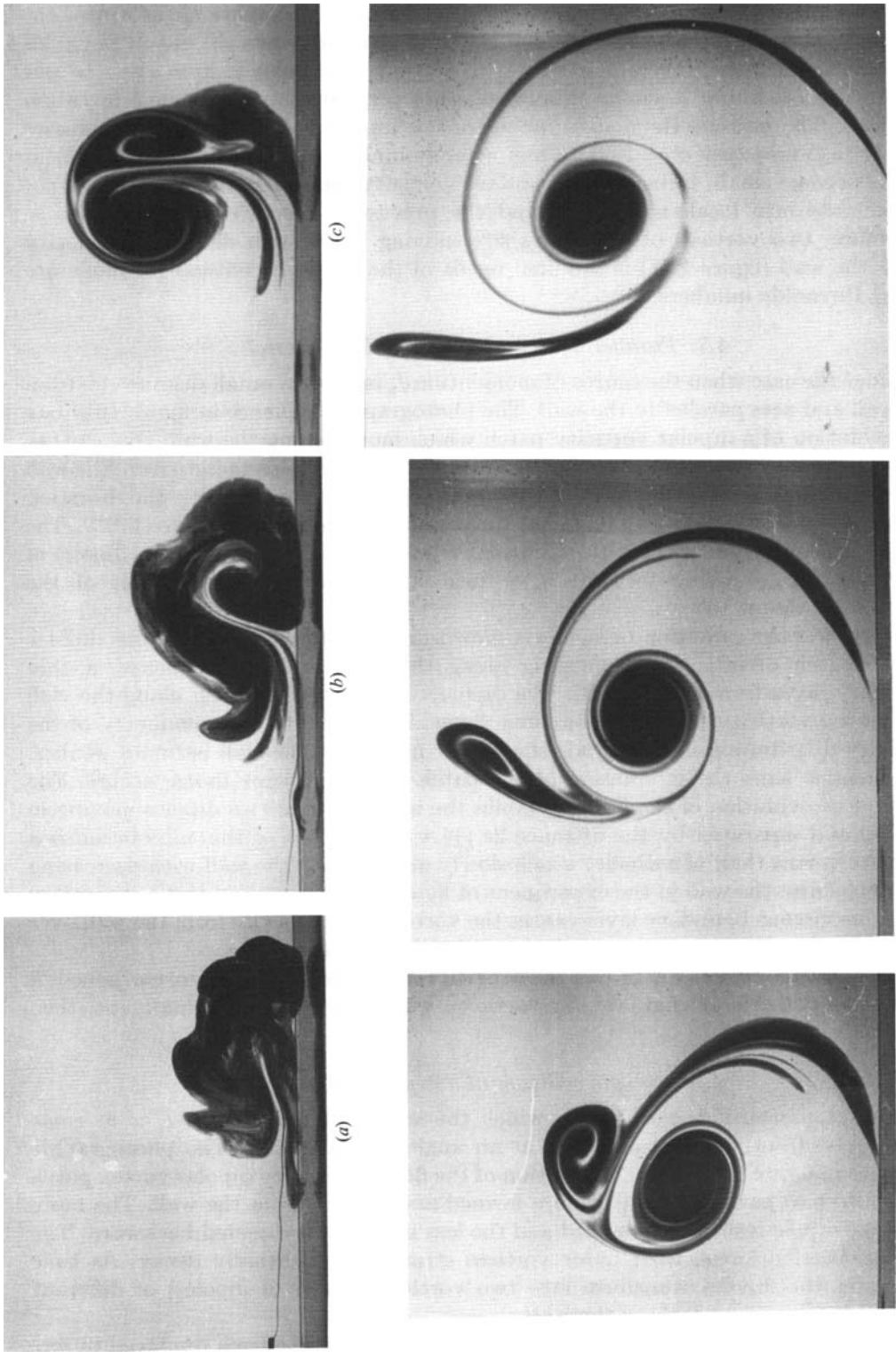

FIGURE 16 (*a–f*). Photographic sequence showing the evolution of an impulsive strong jet ($Re \approx 550$) moving along a wall. Distance between the source and the wall, $\epsilon = 1$ cm. (*a*) $t = 10$ s, (*b*) 24 s, (*c*) 59 s, (*d*) 162 s, (*e*) 320 s, (*f*) 530 s.

(half-dipoles) move apart along the wall. The numerical two-dimensional simulation by Orlandi (1990) shows that the number of intermediate bifurcations, as well as the number of secondary vortices created at the wall, increases when the initial Reynolds number of the flow (the momentum of the primary dipole) is increased. In our experiment the initial Reynolds number was not very large and only one bifurcation occurred. The current Reynolds number of the impulsive vortex dipole decreases with time (Voropayev *et al.* 1991). Thus, after a number of bifurcations the nonlinear effects become small. Hence, the secondary vorticity generated at the wall does not concentrate into localized patches and the process of viscous diffusion prevails. Therefore, two vortices of increasing size moving apart with decreasing velocity along the wall (figure 14*d*) is the final result of the head-on collision for moderate initial Reynolds numbers.

4.7. *Parallel motion of a dipole along the wall.*

Consider the case when the source of momentum I_0 is at some small distance (ϵ) from the wall and acts parallel to the wall. The photographic sequence in figure 16 shows the evolution of a dipolar vorticity patch which moves along the wall. One can see that the dipole forms (figure 16*b*) in a turbulent cloud and then emerges from the wall (figure 16*c*). The eruption of the dipole from the wall resembles the bursting phenomenon in the near-wall region of turbulent boundary layers (Falco 1977). The outer vortex straines and eventually decays. A single vortex (a half of a dipole) of increasing size, moving forward with decreasing velocity, is the result of the interaction (figure 16*f*).

To explain the evolution of the flow shown in figure 16 consider first the dipolar vortex patch of intensity I_0 moving along the wall. As a consequence, a thin boundary layer forms at the wall. The dipolar vortex cloud moving along the wall sweeps the vorticity from the boundary layer. This leads to an asymmetry of the vorticity distribution in the cloud: the vortex nearest to the wall becomes weaker. At the same time the interaction of the patch with its mirror image occurs. The subsequent evolution of the flow resembles the interaction of two dipoles moving in parallel and separated by the distance 2ϵ (§4.4). The result of this interaction is a compact vortex (half of a dipole) which slowly moves along the wall with decreasing velocity. Thus, the wall in the experiment of figure 16 is more than just a symmetry plane: its viscous boundary layer causes the vortex to move away from the wall over a considerable distance (compare figure 16*f* and figure 12*d*).

The question arises, where has the vorticity from the decaying vortex gone? A natural hypothesis is that all the vorticity goes into the vortex tail and then effectively diffuses.

4.8. *Oblique collision of a dipole with a wall*

Finally let us consider the case in which the source of momentum I_0 is at some distance (ϵ) from the wall and acts at an angle α to the wall. The photographic sequence in figure 17 shows the evolution of the flow. A primary dipolar vortex patch splits into two parts: two dipoles are formed and emerge from the wall. The more intensive dipole is directed forward and the less intensive is directed backward. The dipoles describe loops, their outer vortices strain and eventually decay. As time progresses the dipoles transform into two vortices (halves of dipoles) of different intensity moving apart along the wall.

To interpret the evolution of the flow, consider again two effects produced by the wall: the production of vorticity in the boundary layer at the non-slip wall and of

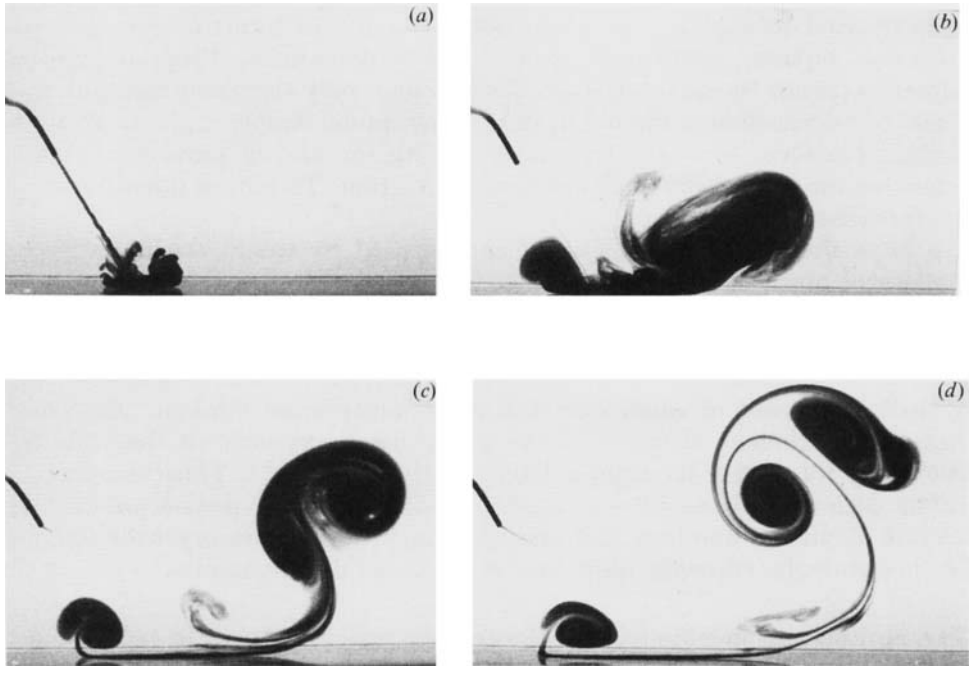

FIGURE 17 (*a–d*). Photographic sequence showing the oblique collision of an impulsive strong jet ($Re \approx 600$) with a wall. Distance between the source and the wall, $\epsilon = 4$ cm. (*a*) $t = 1$ s, (*b*) 15 s, (*c*) 20 s, (*d*) 60 s.

mirror vortices. Both effects influence the flow simultaneously, but for simplicity let us consider them separately. When the source of momentum starts, the induced, potential, dipolar flow causes the emergence of friction forces in the boundary layer at the wall. These forces generate two vortex patches of opposite sign which can be considered as a dipole of intensity I_* directed away from the wall against the source of momentum. Thus, at the intermediate stage, two parameters govern the flow dynamics: $I = I_0 - I_*$ and $Q_* \approx \epsilon I_*$. Owing to the virtual quadrupole, two dipoles form and then move in looping curves in the net, background, dipolar flow of intensity I. At the same time, the mirror image of the flow influences the flow dynamics. Using the same arguments as for an oblique collision of two dipoles (§4.5), we obtain two main parameters governing the flow: $I \cos\alpha$ and $Q = \epsilon I \sin\alpha$. Thus the flow represents the superposition of dipolar and quadrupolar motions and two intermediate dipoles move in this flow. From the geometry, it is clear that the induced velocities combine on the right-hand side of the collision point at the wall and are in opposition on the left-hand side. The right dipole develops in the accompanying background dipolar flow, makes a loop, and transforms into an intense single vortex (this final phase is not shown in figure 17, but it is similar to the last frame in the sequence shown in figure 16). The left dipole develops in the weak background quadrupolar flow, makes a loop and also transforms into a single vortex.

5. Concluding remarks

We have considered a compact vortex quadrupole arising in a viscous fluid from the symmetric collision of two dipoles and explained this result theoretically. We have also reproduced different kinds of vortex-dipole interactions in a stratified fluid

and have tried to explain the interaction dynamics in terms of compact vortex multipoles: dipoles, quadrupoles and their combinations. Proposed governing parameters permit the qualitative prediction of not only the result of an interaction but also of intermediate bifurcations of the flow. In our simple experiments we have restricted ourselves to qualitative analysis with the aim of providing a common perspective for several different kinds of interaction. To obtain quantitative data some further study is needed.

We hope that the results obtained can be used by those who investigate the dynamics of mushroom-like currents in the upper ocean on the basis of satellite images. At first glance, these mesoscale vortex dipoles appear to develop at very high Reynolds numbers, but simple estimates demonstrate that this is not so. A typical horizontal lengthscale (R) of these structures is some tens of kilometres and they exist in a field of small-scale turbulent background motions. The effective background turbulent viscosity in the upper ocean depends on the scale (L) of motion and for $L \ll R$ its typical value is 10^5–10^6 cm^2 s^{-1}. Thus mushroom-like currents with typical velocities of some tens of centimetres per second develop at moderate Reynolds numbers and one may hope that laboratory experiments, at least qualitatively, correctly reproduce real oceanic flow dynamics.

The authors are indebted to Mr I. A. Filippov for his part in performing the experiments and are grateful to Professor G. K. Batchelor and Professor G. I. Barenblatt for helpful discussions and comments.

REFERENCES

Afanasyev, Ya. D. & Voropayev, S. I. 1989*a* A model of the mushroom-like currents in a stratified fluid at the source of momentum acting impulsively. *Izv. Akad. Nauk SSSR, Fiz. Atmos. Okeana.* **25**, 843–851.

Afanasyev, Ya. D. & Voropayev, S. I. 1989*b* On the spiral structure of the mushroom-like currents in the ocean. *Dokl. Akad. Nauk SSSR* **308**, 179–183.

Afanasyev, Ya. D., Voropayev, S. I. & Filippov, I A. 1988 Laboratory investigation of flat vortex structures in a stratified fluid. *Dokl. Akad. Nauk SSSR* **300**, 704–707.

Afanasyev, Ya. D., Voropayev, S. I. & Filippov, I A. 1989 A model of the mushroom-like currents in a stratified fluid when a source of momentum acts continuously. *Izv. Akad. Nauk SSSR, Fiz. Atmos. Okeana.* **25**, 741–750.

Barenblatt, G. I., Voropayev, S. I. & Filippov, I. A. 1989 Model of Fedorovian coherent structures in the upper ocean. *Dokl. Akad. Nauk SSSR* **307**, 720–724.

Batchelor, G. K. 1967 *An Introduction to Fluid Dynamics.* Cambridge University Press.

Cantwell, B. J. 1986 Viscous starting jets. *J. Fluid Mech.* **173**, 159–189.

Couder, Y. & Basdevant, C. 1986 Experimental and numerical study of vortex couples in two-dimensional flows. *J. Fluid Mech.* **173**, 225–251.

Falco, R. E. 1977 Coherent motions in the outer region of turbulent boundary layers. *Phys. Fluids* **20**, 124–132.

Federov, K. N. & Ginzburg, A. I. 1989 *Surface Layer of the Ocean.* Leningrad: Gidrometeoizdat.

Griffiths, R. W. & Hopfinger, E. J. 1984 The structure of mesoscale turbulence and horizontal spreading at ocean fronts. *Deep-Sea Res.* **31**, 245–269.

Heijst, G. J. F. van & Flor, J. B. 1989*a* Laboratory experiments on dipole structures in a stratified fluid. In *Mesoscale/Synoptic Coherent Structures in Geophysical Turbulence* (ed. J. C. J. Nihoul & B. M. Jamart), pp. 591–608.

Heijst, G. J. F. van & Flor, J. B. 1989*b* Dipole formation and collisions in a stratified fluid. *Nature* **340**, 212–215.

Kamke, E. von 1959 *Differentialgleichungen.* Losungsmethoden und losungen. Leipzig.

MANAKOV, S. V. & SCHUR, L. N. 1983 Stochasticity in two-particles dispersion. *Pis'ma V Zh. Tek. Fiz.* **37**, 45–48.

NGUEN DUC, J.-M. & SOMMERIA, J. 1988 Experimental characterization of steady two-dimensional vortex couples. *J. Fluid Mech.* **192**, 175–192.

ORLANDI, P. 1990 Vortex dipole rebound from the wall. *Phys. Fluids* A **2**, 1429–1436.

STERN, M. E. & VOROPAYEV, S. I. 1984 Formation of vorticity fronts in shear flow. *Phys. Fluids* **27**, 848–855.

VOROPAYEV, S. I. 1983 Free jet and frontogenesis experiments in shear flow. *Tech. Rep. Woods Hole Oceanograph. Inst.* WHOI-83-41, pp. 147–159.

VOROPAYEV, S. I. 1987 Modeling of vortex structures in the flow with velocity shear using a jet of variable impulse. *Morskoy Hydrofys. Zh.* **2** (3–4), 33–39.

VOROPAYEV, S. I., AFANASYEV, YA. D. & FILIPPOV, I. A. 1991 Horizontal jets and vortex dipoles in a stratified fluid. *J. Fluid Mech.* **227**, 543–566.

VOROPAYEV, S. I. & FILIPPOV, I. A. 1985 Development of a horizontal jet in a homogeneous and stratified fluids. Laboratory experiments. *Izv. Akad. Nauk SSSR, Fiz. Atmos. Okeana.* **21**, 964–972.

VOROPAYEV, S. I. & NEELOV, I. A. 1991 Laboratory and numerical modelling of vortex dipoles (mushroom-like currents) in a stratified fluid. *Okeanologiya* **31**, 68–75.